

*Exceptional
service
in the
national
interest*

Comparison of Multi-Axis and Single Axis Testing on Plate Structures

85th Shock and Vibration Symposium

Mr. Garrett Nelson, University of Minnesota

Dr. Laura Jacobs-O'Malley, Sandia National Laboratories

October 29th, 2014



U.S. DEPARTMENT OF
ENERGY



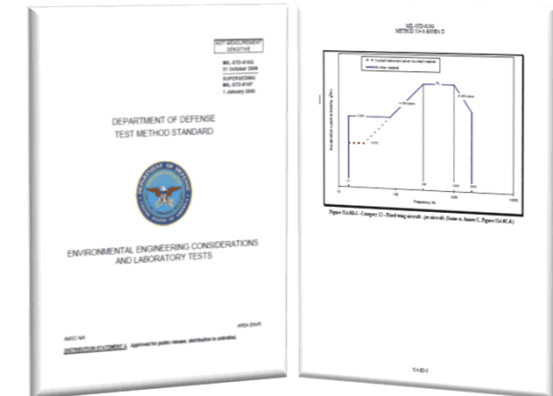
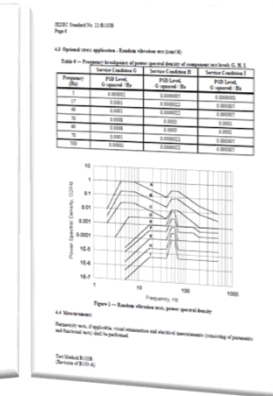
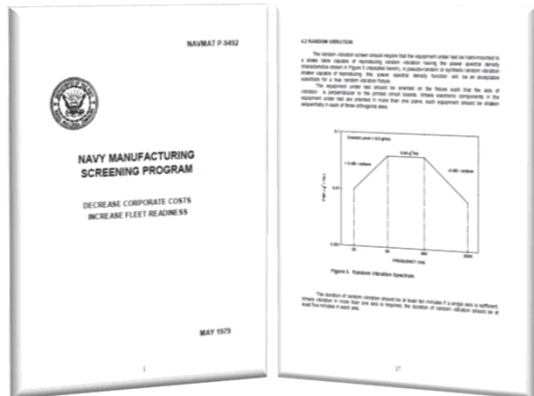
Sandia National Laboratories is a multi-program laboratory managed and operated by Sandia Corporation, a wholly owned subsidiary of Lockheed Martin Corporation, for the U.S. Department of Energy's National Nuclear Security Administration under contract DE-AC04-94AL85000. SAND NO. 2011-XXXXP

Outline

- Motivations & Objective
- Equipment
- Test Article
- Sensor Selection & Configuration
- Test Sequence
 - Axes
 - Levels
 - Coherence and Phase
- Overview of Test Results
 - Energy Levels
 - Peak Accelerations
 - Modal Contributions

Motivations

- Sequential single axis testing has been firmly established as the preferred test method for environmental vibration characterization and analysis
 - MIL STD 810G: U.S. Department of Defense Environmental Test Standard
 - NAVMAT P-9492: U.S. Navy Manufacturing Screening Test Standards
 - JESD22-B103B: JEDEC Environmental Test Standards for Microelectronics



Motivations

- Unfortunately, vibrations in real world environments are 3-dimensional and these vibrations can result in different failure modes and component lifecycles [1-5]
- Recent developments in electrodynamic shaker capabilities have enabled reliable and controllable simultaneous multi-axis testing [6,7]
- Multi-axis control makes possible true single axis testing by allowing control of off axis and rotational vibrations that may be present in uniaxial shakers [8]
- Model validation and system identification via single axis test results cannot account for off axis affects [9]

Objective

- Through a collaboration of experimental and modeling work conducted on a given test article investigate:
 - The relationship between single axis and multi-axis vibration testing
 - How are fatigue life estimates influenced by stimulation from more than one axis?
 - Can results from a single axis test be used to predict multi-axis results for a given part structure?
 - What's the effect of multi-axis inputs on a test article's modal response?
 - The effect of coherence and/or phase relationships on the energy levels experienced by a part during biaxial or triaxial vibration testing
 - The benefit of single axis testing conducted on equipment capable of mitigating off-axis (and rotational) vibration

Test Equipment

- Shaker System: Team Corporation Tensor™ 900



- Simultaneous or sequential excitation of X, Y, and/or Z axes
- Complete control of rotations around all axes

Specifications

Table First Frequency	5,000 Hz
Test Frequency Range	10 - 5,000 Hz
Max Payload	9 lbs
Max Displacement	0.5 in
Max Acceleration (w/max payload)	10 g



- Controller Software: Spectral Dynamics JAGUAR Shaker Control and Analysis System

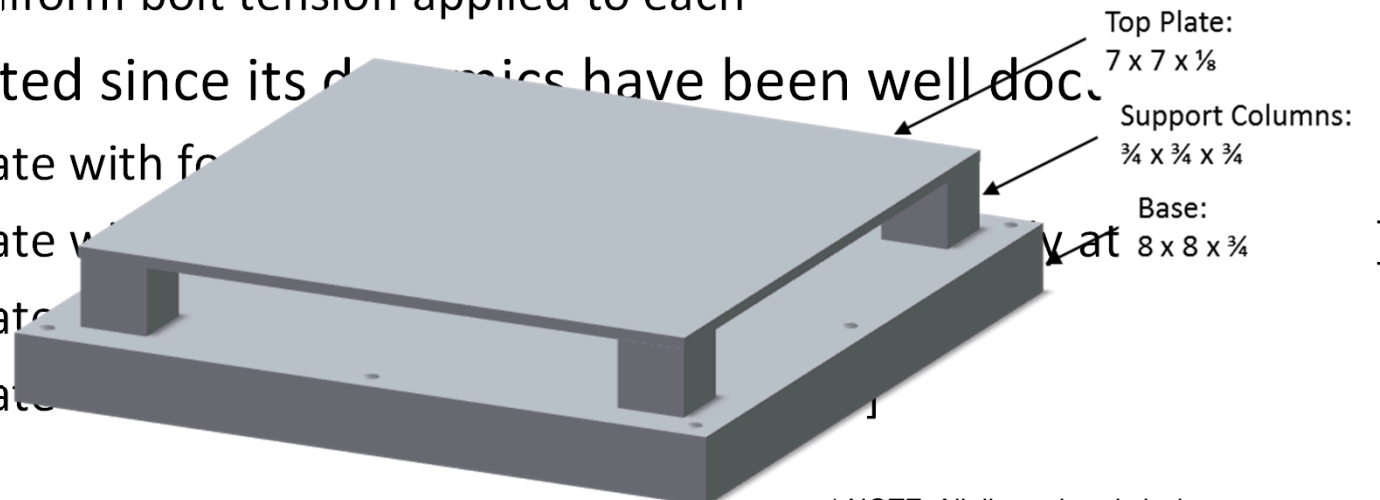


- Multi-Input and Multi-Output Control
- Input and Output Transformation for 6DOF Control
- Data Acquisition: National Instruments™ LabVIEW and NI PXIe-4496 Data Acquisition Modules



Test Article

- A column supported square aluminum 6061 plate
 - Base, columns, and top plate made of a continuous piece of material
 - Both homogenous and isotropic
 - Eliminates added dynamics due to support boundaries
- Evenly spaced mounting holes
 - Eight (8) circumferential and one (1) central
 - Uniform bolt tension applied to each
- Selected since its dynamics have been well doc.

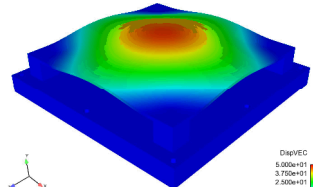


* NOTE: All dimensions in inches

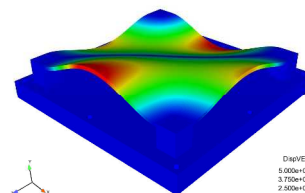
Test Article

- Finite Element Model
 - Used to predict dominant mode shapes and frequency components
 - Confirms that support columns are not dynamically active in frequency range of interest
- Primary Mode Shapes Identified

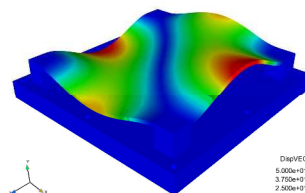
506 Hz



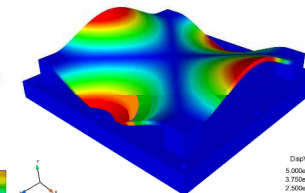
856 Hz



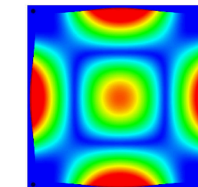
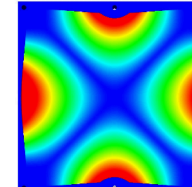
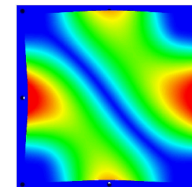
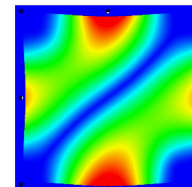
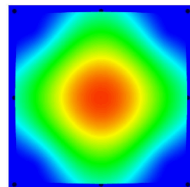
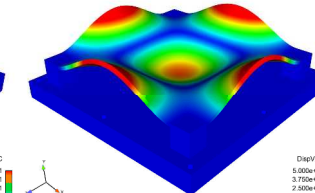
856 Hz



936 Hz



1407 Hz

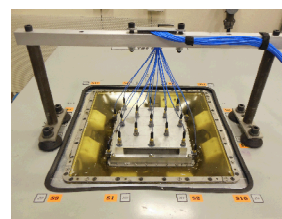
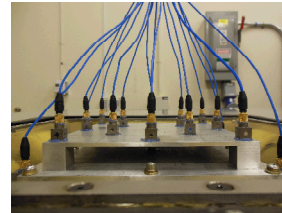
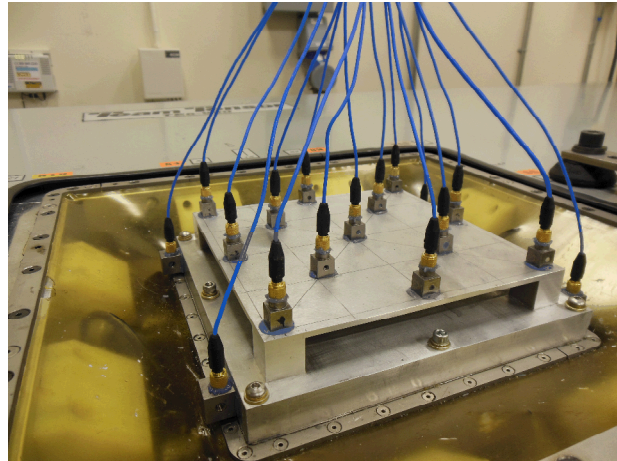


Sensor Selection & Configuration

- Control Accelerometers

- PCB 356A15

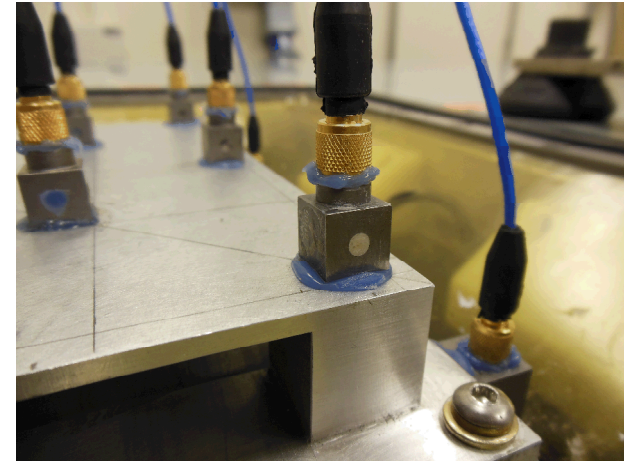
- Triaxial ICP Accelerometer
 - Nominal Sensitivity: 100 mV/g
 - Weight: 0.37 oz



- Response Accelerometers

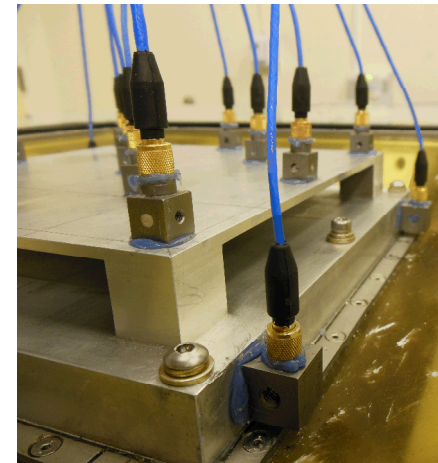
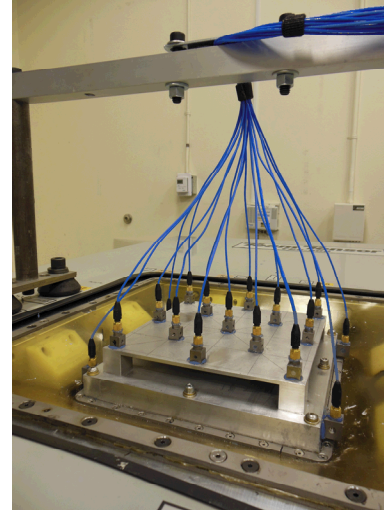
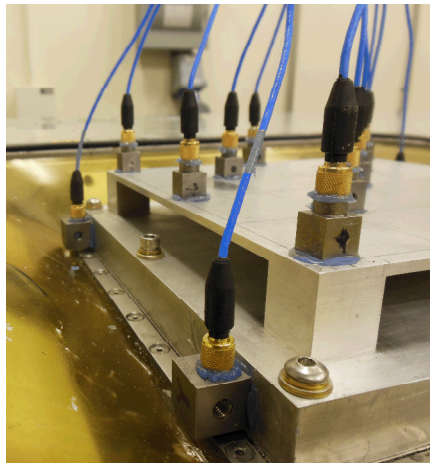
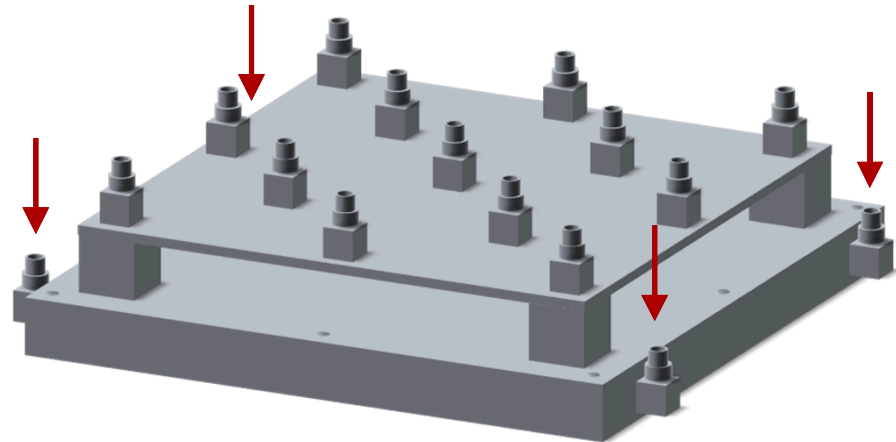
- PCB 356A33

- Triaxial ICP Accelerometer
 - Nominal Sensitivity: 10 mV/g
 - Weight: 0.19 oz



Sensor Selection & Configuration

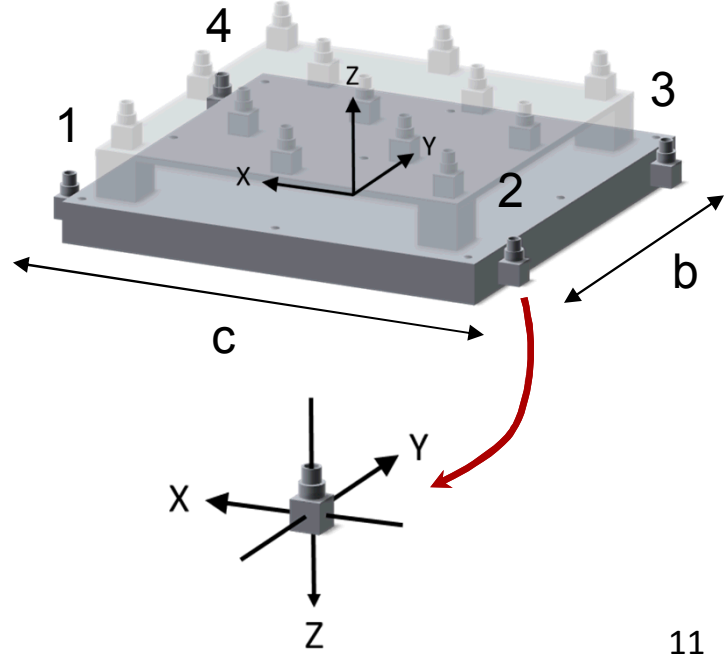
- Control Sensor Placement
 - Symmetric about both lateral axes on base
 - Allows calculation of all base translational and rotational degrees of freedom



Sensor Selection & Configuration

- Control Transformation
 - Given the acceleration from triaxial control accelerometers
 - Calculate the base input translational and rotational acceleration [14]
 - $\vec{A} = H\vec{a}$

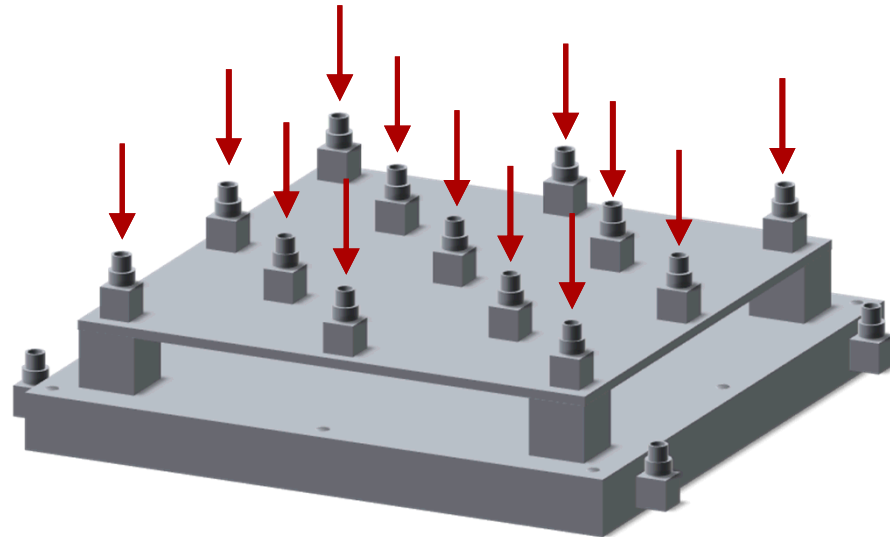
$$\begin{bmatrix} A_X \\ A_Y \\ A_Z \\ A_\Psi \\ A_\Theta \\ A_\Phi \end{bmatrix} = \begin{bmatrix} \frac{1}{4} & 0 & 0 & \frac{1}{4} & 0 & 0 & \frac{1}{4} & 0 & 0 & \frac{1}{4} & 0 & 0 \\ 0 & \frac{1}{4} & 0 & 0 & \frac{1}{4} & 0 & 0 & \frac{1}{4} & 0 & 0 & \frac{1}{4} & 0 \\ 0 & 0 & -\frac{1}{4} & 0 & 0 & -\frac{1}{4} & 0 & 0 & -\frac{1}{4} & 0 & 0 & -\frac{1}{4} \\ 0 & 0 & -\frac{g_0}{2b} & 0 & 0 & \frac{g_0}{2b} & 0 & 0 & \frac{g_0}{2b} & 0 & 0 & -\frac{g_0}{2b} \\ 0 & 0 & -\frac{g_0}{2c} & 0 & 0 & -\frac{g_0}{2c} & 0 & 0 & \frac{g_0}{2c} & 0 & 0 & \frac{g_0}{2c} \\ -\frac{g_0}{4b} & -\frac{g_0}{4c} & 0 & \frac{g_0}{4b} & -\frac{g_0}{4c} & 0 & \frac{g_0}{4b} & \frac{g_0}{4c} & 0 & -\frac{g_0}{4b} & \frac{g_0}{4c} & 0 \end{bmatrix} \begin{bmatrix} a_{x_1} \\ a_{y_1} \\ a_{z_1} \\ a_{x_2} \\ a_{y_2} \\ a_{z_2} \\ a_{x_3} \\ a_{y_3} \\ a_{z_3} \\ a_{x_4} \\ a_{y_4} \\ a_{z_4} \end{bmatrix}$$



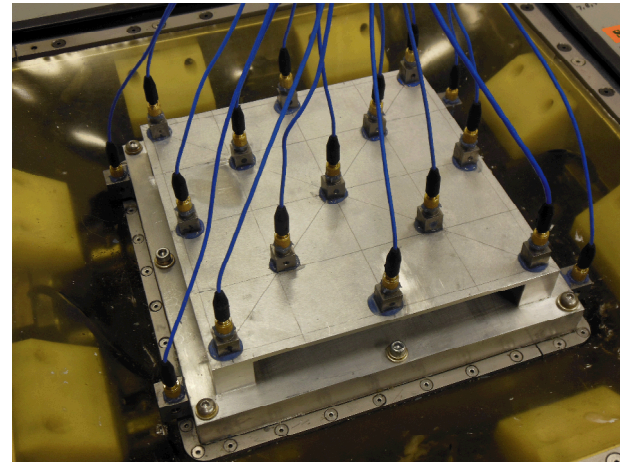
 \vec{A} H \vec{a}

Sensor Selection & Configuration

- Reference Sensor Placement:
 - Center of plate
 - Each corner
 - Mid-span of each side
 - Along each diagonal placed evenly between the center and corner accelerometers



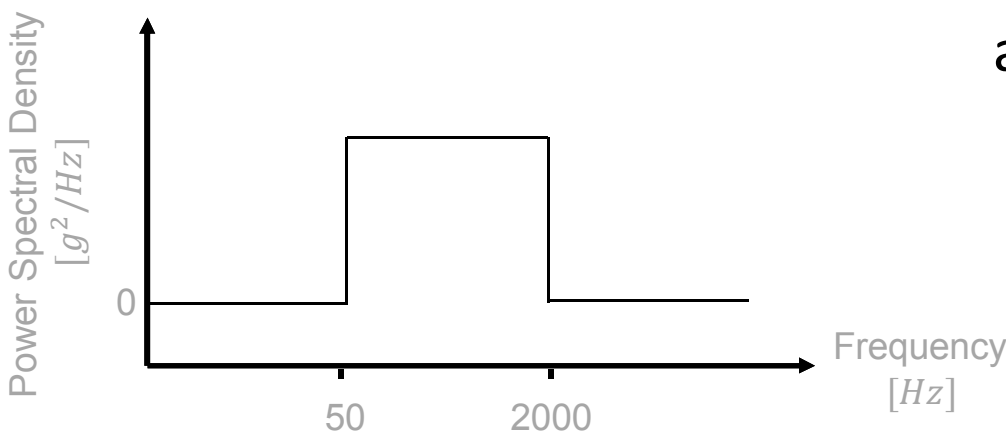
- The high number of accelerometers caused a mass loading affect on the top plate
- Their positions were selected to mitigate mode shape distortion
- FEA data confirms that modes are preserved although all frequencies were shifted lower



Test Sequence

- Control Signal
- Axes
- Input Level
- Cross-Axis
- Coherence & Phase

- Band-limited white noise (50Hz – 2kHz)
- Causes simultaneous excitation of all frequencies within range
- All frequency dependence in stimulated responses can be attributed to plate dynamics

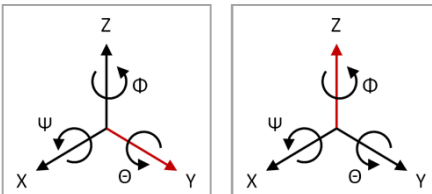
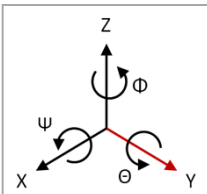
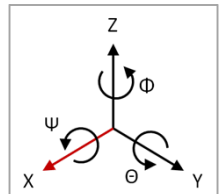


Test Sequence

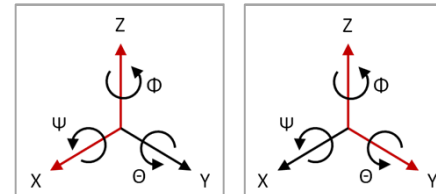
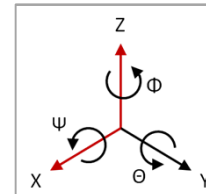
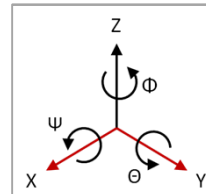
- Control Signal
- Axes
- Input Level
- Cross-Axis
- Coherence & Phase

- Single and Multi-Axis
 - Uniaxial: One translational axis at a time (X, Y, Z)
 - Biaxial: Two translational axes at a time (XY, XZ, YZ)
 - Triaxial: All three axes simultaneously (XYZ)
- All axes always controlled, but not all to full test levels

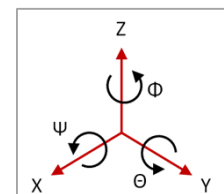
Uniaxial



Biaxial



Triaxial

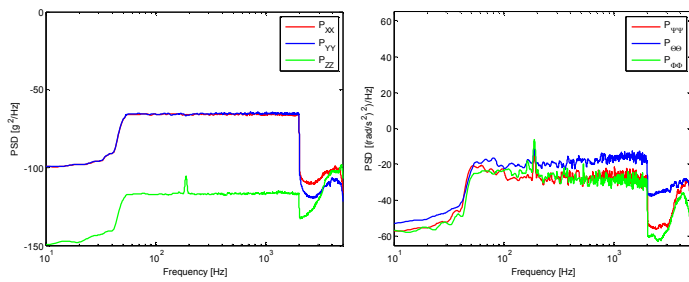


Test Sequence

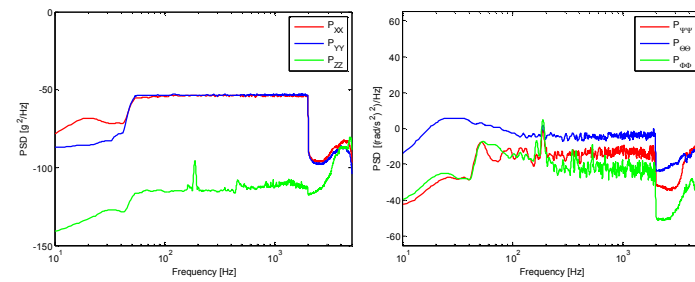
- Control Signal
- Axes
- Input Level
- Cross-Axis Coherence & Phase

- Input Acceleration Levels: low ($1g_{rms}$) & high ($2g_{rms}$)
- Same acceleration level for all applicable axes
- All other DOFs controlled to low level

X & Y Translation Controlled (@ 1g)
Z Translation & All Rotations Minimized

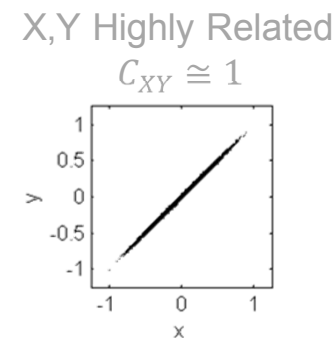
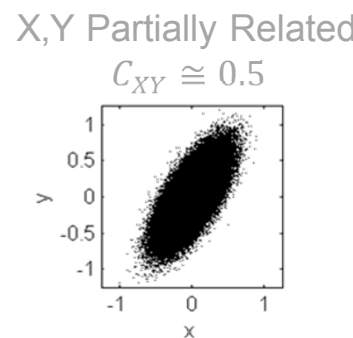
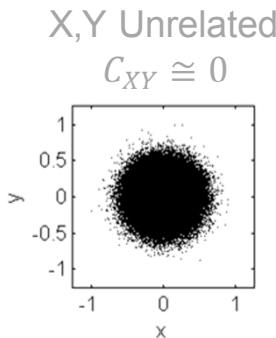


X & Y Translation Controlled (@ 2g)
Z Translation & All Rotations Minimized



Test Sequence

- Control Signal
- Axes
- Input Level
- Cross-Axis Coherence & Phase
 - Zero phase between all axes
 - Coherence is measure of relationship between two signals
 - Levels: low (~ 0), medium (0.50), and high (~ 1)
 - Coherence with and between all other DOFs set at zero



Response Energy

- $e = e_x + e_y + e_z$
 - Where, $e_n = \frac{1}{L} \sum_{j=1}^L v_n[j]^2 \quad \{\forall n = x, y, z\}$
- The energy of the i^{th} response accelerometer ($e_{R_n[i]}$) was normalized by the energy of the control input (e_C)
 - $e'_{R_n[i]} = e_{R_n[i]} / e_C$
 - This accounts for the known input energy level differences between single and multi-axis test cases
- Then, the total normalized energy of the response accelerometers is given by
 - $E'_n = \sum_{i=1}^N e'_{R_n[i]} \quad \{N = 13 \text{ (total number of response accels)}\}$

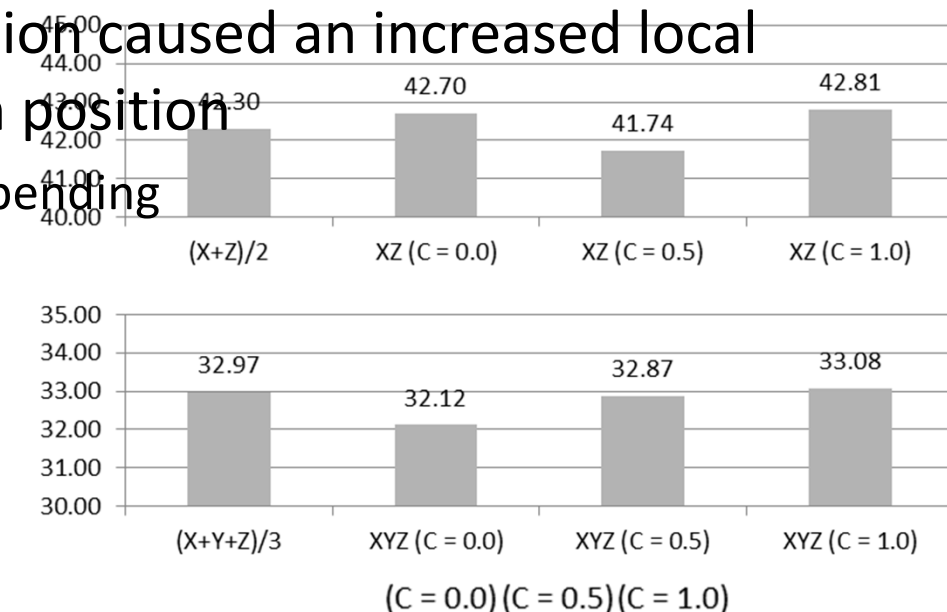
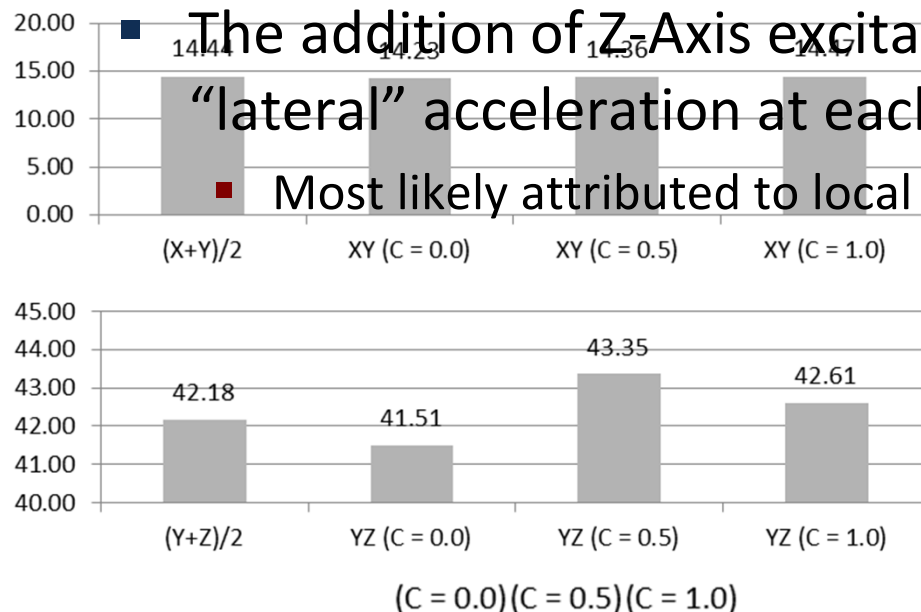
Response Energy

- Total normalized energy levels are comparable between multi-axis
- Total normalized energy levels are comparable between approximating multi-axis tests
- Total normalized energy levels are comparable between single axis

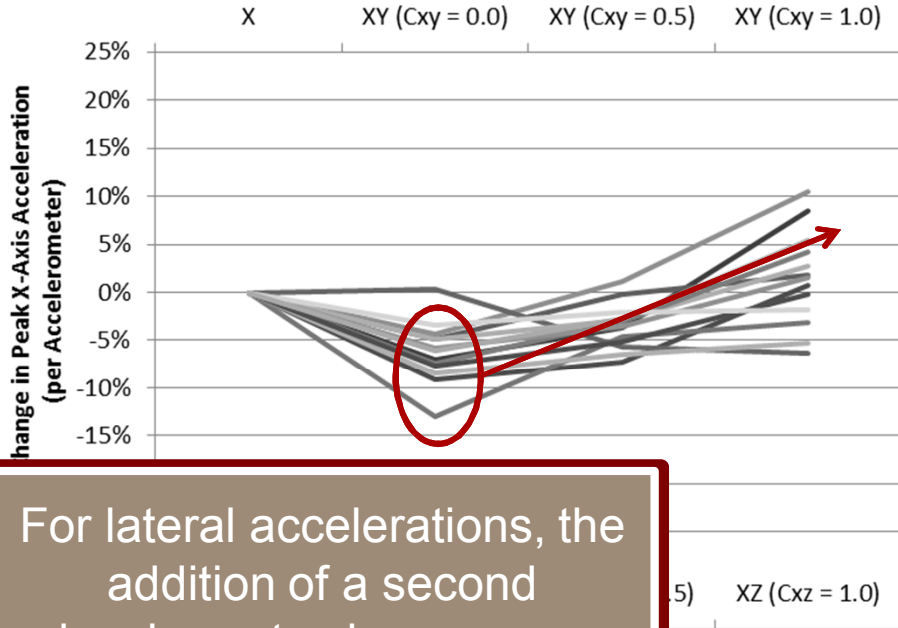
This estimate was bounded by the maximum and minimum energy levels for multi-axis tests

..

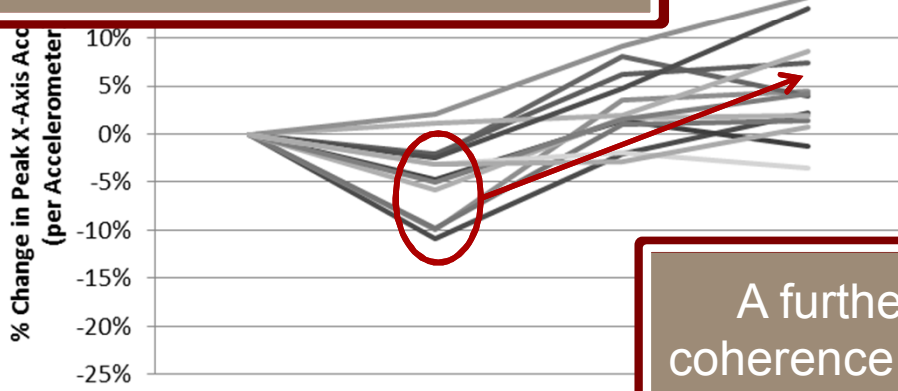
It can't serve as either a reliable upper or lower bound for anticipated multi-axis energy levels



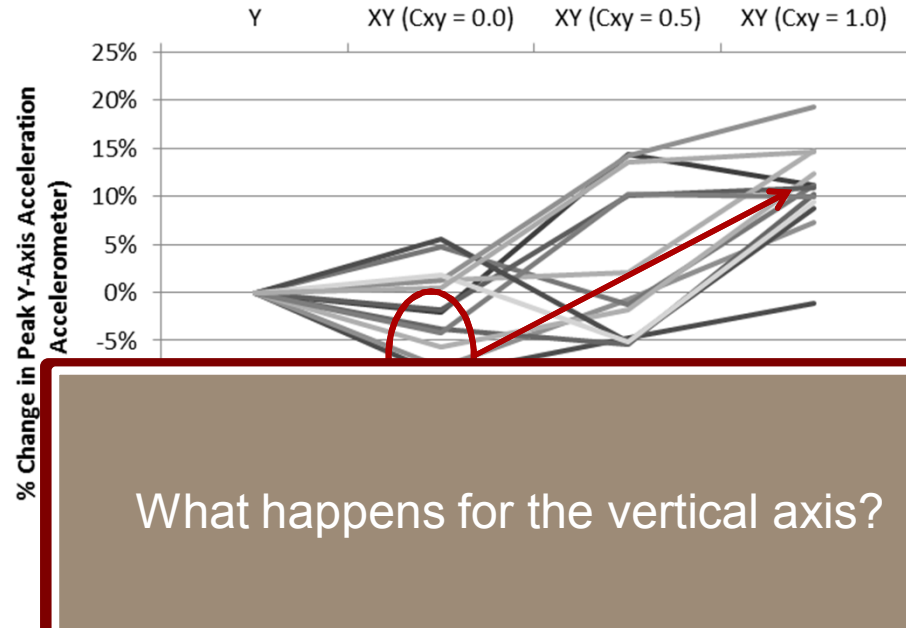
Peak Acceleration



For lateral accelerations, the addition of a second incoherent axis causes a decrease in peak acceleration



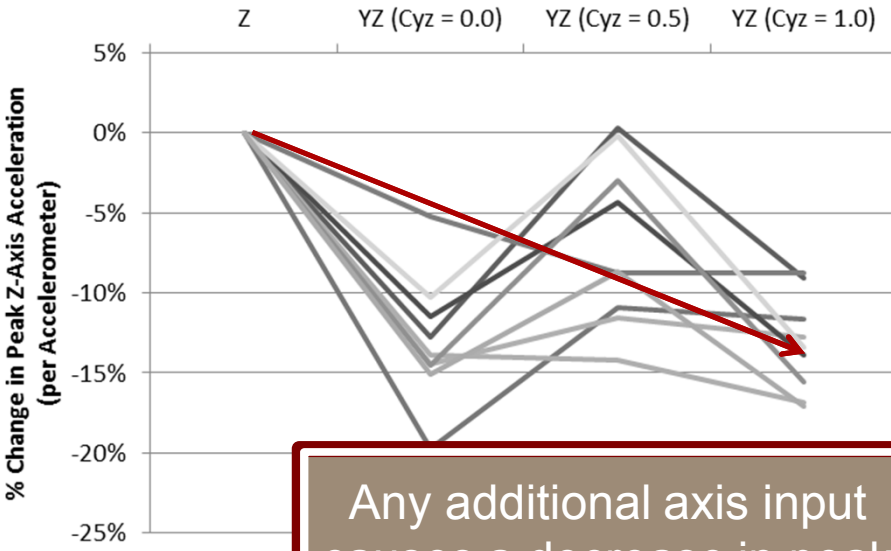
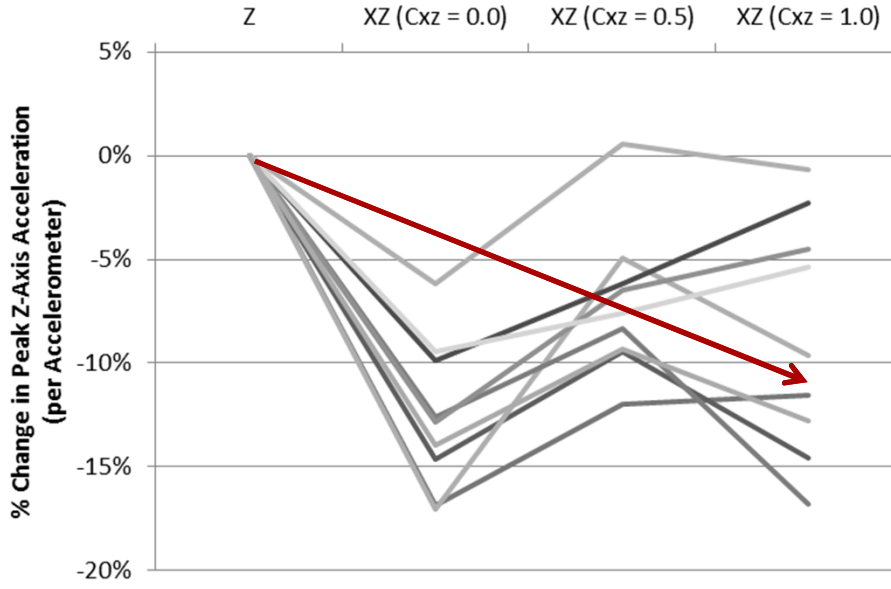
A further increase in coherence raises the peak levels



What happens for the vertical axis?

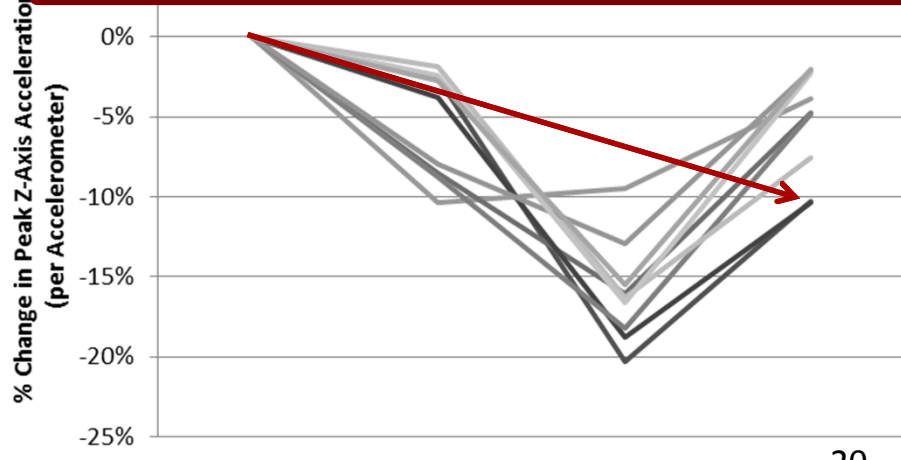


Peak Acceleration



Any additional axis input causes a decrease in peak acceleration levels

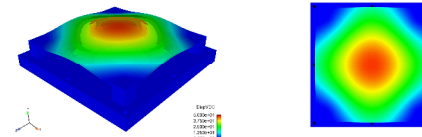
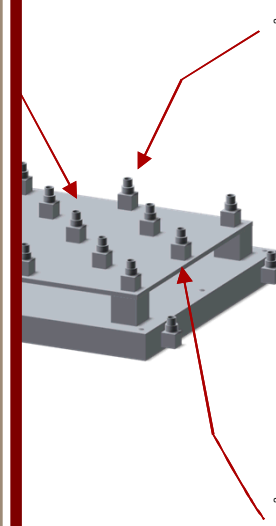
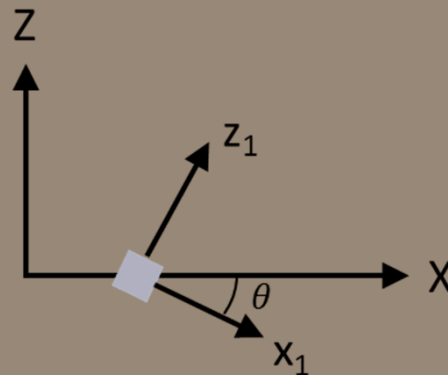
What happens for the vertical axis?



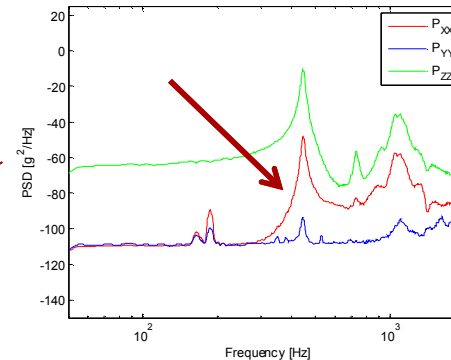
Modal Response

- Responses for each test dominated by first mode shape

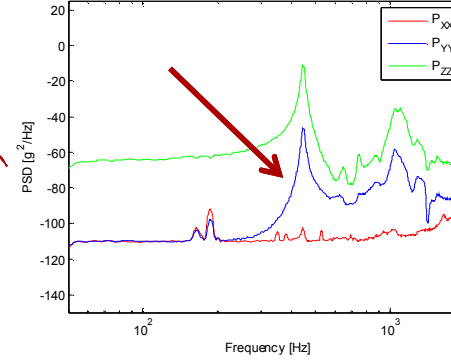
For edge accelerometers, the observed lateral response is due to plate bending. For a bent plate, a portion of the global z-axis acceleration appears locally as a x or y-axis acceleration



X Edge Accelerometer

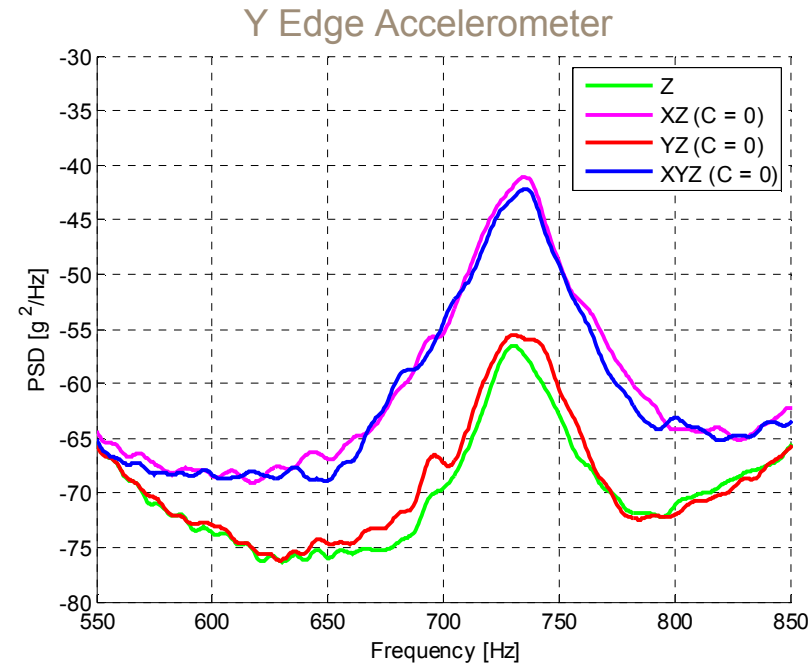
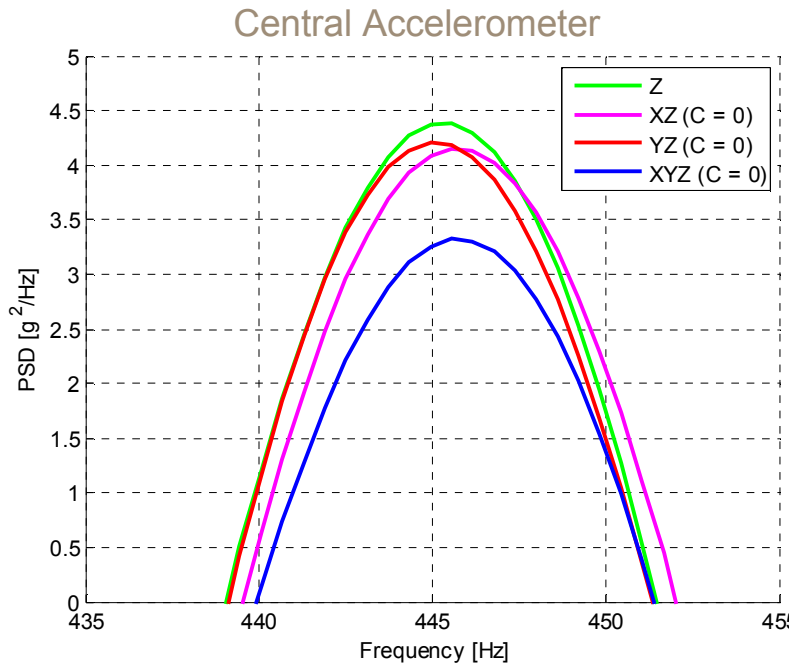


Y Edge Accelerometer



Modal Response

- Dominant frequencies remain constant, but modal contribution changes depending on excitation level of additional axes



Conclusions

- For a plate structure, uniaxial testing in line with the dominant axis results in worst case testing
- For conservative fatigue or life-cycle testing, peak response axis must be known a-priori
- Even for simple structures, modal contribution is altered by multi-axis testing
 - Corresponding stress state will never be captured by single axis tests
- On uniaxial shakers, presence of off axis stimuli due to internal coupling may distort results
 - True single axis testing can only be performed on multi-axis shaker
 - Control of off axis contributions can enable improved model validation
- Combined single axis response data cannot accurately be used to predict or bound multi-axis scenarios

References

- [1] R.M. French, R. Handy, and H.L Cooper, "A comparison of simultaneous and sequential single-axis durability testing," *Experimental Techniques*, vol. 30, no. 5, pp. 32-37, Sept./Oct. 2006.
- [2] D.L. Gregory, F. Bitsie, and D.O. Smallwood, "Comparison of the response of a simple structure to single axis and multiple axis random vibration inputs," in *Proc. 80th Shock and Vibration Symp.*, San Diego, CA, Oct. 2009.
- [3] E. Habtour et al., "Improved reliability testing with multiaxial electrodynamics vibration," in *Proc. 2010 Reliability and Maintainability Symp.*, San Jose, CA, pp. 1-6, Jan. 2010.
- [4] B. Aytekin and H.N. Ozguven, "Vibration analysis of a simply supported PCB with a component - an analytical approach," in *Proc. 10th Electronics Packaging Technology Conf.*, Singapore, pp. 1178-1183, Dec. 2008.
- [5] W.E Whiteman, "Multiaxial versus uniaxial vibration testing: a research plan for comparison," in *19th Int. Modal Analysis Conf.*, Orlando, FL, Feb. 2001.
- [6] D.O. Smallwood and D.L. Gregory, "Evaluation of a 6-DOF electrodynamic shaker system," in *Proc. 79th Shock and Vibration Symp.*, Orlando, FL, Oct. 2008.
- [7] D.J. Osterholt, N.C. Yoder, and D. Linehan, "Advances in six degree of freedom vibration testing," in *Proc. Experimental and Appl. Mechanics*, June 2007.

References

- [8] K.Y. Chang and A.M. Frydman, "Three-dimensional random vibration testing definition and simulation," in *Proc. 36th Annual Mtg. Institute of Environmental Sciences*, Mount Prospect, IL, pp. 129-139, 1990.
- [9] U. Fullekrug and M. Sinapius, "Structural dynamics identification by means of multi-axial base excitation - theory and application," in *Proc. European Conf. on Spacecraft Structures, Materials, and Mechanical Testing*, Braunschweig, Germany, pp. 503-509, Nov. 1998.
- [10] R.D. Blevins, "Plates," in *Formulas for Natural Frequency and Mode Shape*, Malabar, FL: Krieger, Jan. 2001, pp. 264-269.
- [11] D.J. Johns and R. Nataraja, "Vibration of a square plate symmetrically supported at four points," *J. of Sound and Vibration*, vol. 25, no. 1, pp. 75-82, Nov. 1972.
- [12] M.B. Felemban, "Vibration analysis of point and column supported mindlin plates," M.S. thesis, Mech. Eng., King Fahd Univ. of Petroleum & Minerals, Dharan, Saudi Arabia, 1989.
- [13] M. Petyt and W.H. Mirza, "Vibration of column-supported floor slabs," *J. of Sound and Vibration*, vol. 21, no. 3, pp. 355-364, Apr. 1972.
- [14] M.A. Underwood and T. Keller, "Applying coordinate transformations to multi-DOF shaker control," *Sound and Vibration*, vol. 40, no. 1, pp. 22-27, Jan. 2006.

Thank you for your attention!

QUESTIONS?